Deficiency of ValRS-m Causes Male Infertility in Drosophila melanogaster

Xin Duan , Hao Lin Wang , Zhi Xian Cao , Na Su , Yu feng Wang , Ya Zheng *

Posted Date: 10 May 2024

doi: 10.20944/preprints202405.0712.v1

Keywords: ValRS-m ; ; Drosophila melanogaster ; ; mitochondria ; ; spermatogenesis ; ; meiosis

 doi:10.20944/preprints202405.0712.v1

Article

Deficiency of *ValRS-m* Causes Male Infertility in *Drosophila melanogaster*

Xin Duan [1], Hao-Lin Wang [1], Zhi-Xian Cao [1], Na Su [2], Yu-Feng Wang [1] and Ya Zheng [2,*]

[1] School of Life Sciences, Central China Normal University, Wuhan 430079, China.
[2] School of Life Sciences, Shanghai Normal University, Shanghai, 200234, China,
* Correspondence: zhengyahb@shnu.edu.cn

Abstract: The *Drosophila* spermatogenesis has the renewal of germline stem cells, meiosis of spermatocytes, and morphological transformation of spermatids into mature sperm. We previously demonstrated that Ocnus (ocn) plays an essential role in spermatogenesis. *ValRS-m* (*Valyl-tRNA synthetase, mitochondrial*) gene was downregulated in *ocn* RNAi testes. By hatchability testing, we found that *ValRS-m*-knockdown induced complete sterility of male flies. We also concluded that *ValRS-m*-knockdown inhibited the transition from spermatogonia to spermatocytes and caused accumulated spermatogonia in testes. To understand the intrinsic reason for this destruction, we further conducted transcriptome sequencing analysis in *ValRS-m* RNAi testes. A total of 7710 differentially expressed genes (DEGs) were identified to have at least a 2-fold change with a *p*-value of <0.05, including 4725 down-regulated genes (dDEGs) and 2985 up-regulated genes(uDEGs). The dDEGs are mainly concentrated in glycolytic pathway and pyruvate metabolic pathway, and uDEGs are primarily related to ribosomal metabolic pathway. We also confirmed that six meiosis-related genes expression reduced significantly in *ValRS-m* RNAi testes. 28 DEGs associated with mitochondria were verified to be suppressed when *ValRS-m* was insufficient. These results suggest that *ValRS-m* play widely and vital role in the mitochondrial function and male germ cells differentiation during spermatogenesis.

Keywords: *ValRS-m*; *Drosophila melanogaster*; mitochondria; spermatogenesis; meiosis

1. Introduction

Recent studies have shown that up to 10-15% of human couples in the world are currently infertile, and about 30%-40% of these cases are due to male infertility factors, including asthenospermia and oligospermia [1]. Multiple genetic manipulation tools in *Drosophila* melanogaster provide a significant opportunity to study conserved signaling pathways during spermatogenesis [2]. The spermatogenesis of *Drosophila* mainly includes germline stem cells renewal, primary spermatocyte meiosis and spermatocyte-to-sperm morphological transformation [3]. In the spermatocyte, each germline stem cells (GSC) divides asymmetrically to create two daughter cells, one daughter cells attached to the central cells to maintain its stem cells characteristics, and the other daughter cells, called the spermatogonium (GB), enters the differentiation process, and one GB undergoes four mitosis to create 16 spermatogonia cells, which grow into the primary spermatocytes (16S). It then undergoes two meiosis to create 64 round sperm cells connected by intercytoplasmic bridges. The sperm cells in the cyst undergo lengthening and individualization, eventually becoming haploid mature sperm, after which they coil and enter the spermatocyst until fertilization occurs [4].

The balance between animal germ cells proliferation and differentiation is critical for germline homeostasis. It is tightly regulated by stem cells niche and spermatogonial transit-amplification (TA) division [5]. Germline differentiation must be coordinated with GSCs self-renewal, and spermatogonium must undergo meiosis at the right time [6]. Previous studies have shown that transcriptional activation is the primary mechanism of mitosis to meiosis transition, and the expression of multiple genes is changed during the transition from S16 to primary spermatocyte [7]. Activation of tMAC (testis-specific meiotic arrest complex) promotes spermatocyte meiosis [8,9]. The mutation of *aly* gene, as one of the tMAC members, could result in a rich spermatocyte in the testes and abnormal spermatocyte differentiation, thus eventually male infertility [10].

 doi:10.20944/preprints202405.0712.v1

Recent studies have shown significant mitochondrial recombination during TA transformation in *Drosophila* spermatogenesis [11]. In the early stages of spermatogenesis in many insects, the number and appearance of mitochondria are similar to those of somatic cells, dispersed in the cytoplasm. In the primary spermatocyte before meiosis, the mitochondria cluster near the nucleus and present a spherical structure. After meiosis II is completed, hundreds of mitochondria fuse into two long mitochondrial derivatives, which intertwine to form a spherical aggregate near the nucleus, known as the accessory nucleus (nebenkern). During the elongation of sperm cells, the behavior of mitochondrial derivatives also changes, in which the contents of major derivatives are relatively dense, while the volume of minor derivatives decreases and there is no accumulation of contents [12]. *Drosophila fzo* was first discovered as a mitochondrial dynamic gene, belongs to one member of the evolutionally-conserved mitochondrial fusion protein family (Mfns), encoding a sizeable transmembrane GTPase associated with dynamin that mediates mitochondrial fusion during spermatogenesis. Deletion of the *Fzo* (fuzzy onions) gene causes the mitochondria to fail to fuse properly, resulting in the formation of malformed nebenkern and male sterility [13].

The human gene *VARS2* (*Valyl-tRNA synthetase 2*) is related to *COXPD20* (*combined oxidative phosphorylation deficiency 20*) [14]. Studies have shown that *VARS2* mutation can cause autosomal recessive mitochondrial encephalomyopathy [15,16]. *VARS2* mutations can also lead to varying degrees of developmental delay, axial hypotonia, limb spasms, and even premature death [17]. The homolog of *VARS* in flies is *ValRS-m* gene, located on mitochondria, and highly expressed in the testis. Notably, we have previously found that the knockdown of *ocnus* which encoding histidine phosphatase in fly testis can lead to abnormal development of testis and male sterility [18]. Through comparative proteomics detection, ValRS-m protein was significantly down-regulated in *ocn* knock-down fly testes. However, its specific function in *Drosophila* has not been reported so far.

In the present study, we explored the role of *ValRS-m* in *Drosophila* spermatogenesis. *ValRS-m* knockdown in testes caused male sterility and early spermatogenesis defects in files. *ValRS-m*-knockdown testes exhibited severe defects in spermatocyte differentiation. Immunofluorescence staining and electron microscopic examination revealed *ValRS-m*-knockdown disrupts the mitochondrial fusion and ATP synthesis, excessive apoptosis occurs in *ValRS-m*-knockdown testes. Together, these findings indicated that *ValRS-m* is required in *Drosophila* spermatogenesis by controlling mitochondrial dynamics and function in spermatocyte differentiation. Our results can not only further understand the regulatory mechanism of animal reproductive development, but also provide a valuable theoretical reference for the further study of human spermatogenesis and mitochondrial diseases.

2. Results

2.1. Knockdown of ValRS-m in Testes Caused Male Infertility

Due to *ValRS-m* was decreased significantly in ocn knockdown testes that has failure spermatogenesis [18], to explore the role of *ValRS-m* in *Drosophila* male fertility, its expression levels in one day old testes and ovaries were detected by qRT-PCR. As shown in Figure 1A, the transcript of *ValRS-m* was considerably higher in the testis than in the ovary. To further examine the role of *ValRS-m* in male fertility, the UAS-Gal4 system was adopted to manipulate the expression levels of *ValRS-m* in fly testis. It is known that bag-of-marbles (bam) is expressed in spermatogonia as a critical regulator of spermatogonia proliferation and becomes silenced in the spermatocytes [19]. By crossing UAS-*ValRS* RNAi male flies with bam-gal4 females, *ValRS-m* was knocked down specifically in spermatogonia of the male offspring (bamGal4>ValRS-m-hp). The knockdown efficiency of *ValRS-m* expression in these testes was validated by qRT-PCR (Figure 1B). To assess whether knockdown of *ValRS-m* in fly testes may affect male fertility, we crossed the 1-day-old *ValRS-m* RNAi males with 3-day-old w1118 virgin females and collected the eggs. Surprisingly, in three independent trials, the hatch rates of the eggs in cross groups with *ValRS-m* RNAi males were zero. In contrast, 89.57 ± 0.35% of eggs from the crosses with control males hatched (Figure 1C). These results indicated that *ValRS-m* is required for male fertility.

 doi:10.20944/preprints202405.0712.v1

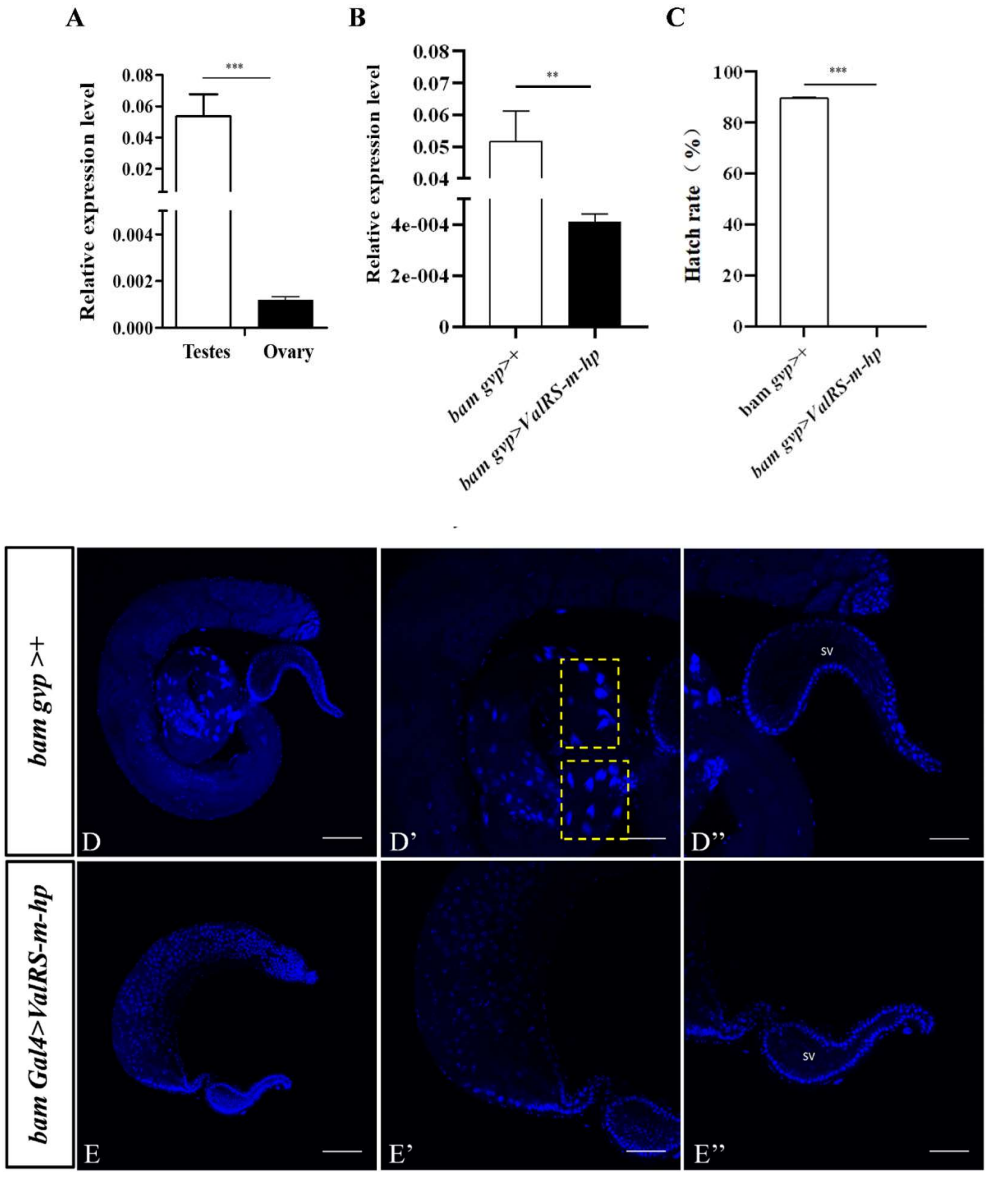

Figure 1. Knockdown of *ValRS-m* in testes caused *Drosophila* male infertility. (**A**) The *ValRS-m* expression levels in one day old adult testes was significantly increased than that in ovaries by qRT-PCR. (**B**) The *ValRS-m* expression level was significantly reduced in *Bam Gal4>ValRS-m-hp* (*ValRS-m* RNAi) testes. (**C**) The hatch rate of eggs from the cross of wild-type females and *ValRS-m* RNAi males was zero. **P*<0.05; ** *P*<0.01; *** *P*<0.001. The immunofluorescent staining using DAPI for spermatogenesis in control testis (**D-D''**) and *ValRS-m*-knockdown testis (**E-E''**). D and E are the whole testes. D′ and E' are the areas where sperm clusters (indicated by arrowheads) are located. D'' and E'' are the seminal vesicles (SV). D′ and E′ are parts of the enlarged area of D and E. the yellow boxes represent sperm clusters. DNA was stained with DAPI (blue). Many mature acicular sperm nuclei are visible in the SV of the control group (**D''**), but no sperm nuclei are visible in the SV of the knockdown testes (**E''**). DNA was stained with DAPI (blue). Scale bars, 100 μm (D, E); 50 μm (D′, D'', E′, E'').

Then, we dissected these adult testes and checked the spermatogenesis progress in these flies. DNA staining could mark the early-stage nuclei at the apex of the testis and the nuclei of clusters of elongated spermatozoa at the tail of the testis [20]. The testes were stained with DAPI and we firstly found that, the size of *ValRS-m* RNAi testes became more minor than the control testes (Figure 1D, E). Secondly, comparing that in the control testes, the sperm bundles were cone-shaped and the sperm nuclei were concentrated, however, navicular nuclei and sperm bundles were disappeared in the *ValRS-m* knockdown testes (Figure 1D′, E′). Finally, a large of mature sperm were scattered in the

 doi:10.20944/preprints202405.0712.v1

seminal vesicles of the control testes. In contrast, no mature sperm was found in the seminal vesicles of the *ValRS-m* RNAi testes (Figure 1D'', E''). Taken together, these results suggested that the knockdown of *ValRS-m* in spermatogonia led to the severe defects in male infertility.

2.2. ValRS-m RNAi Inhibits Spermatogonia Differentiation and Caused Abnormal Proliferation

To further explore the roles of *ValRS-m* during male fertility, we analyzed morphological changes of germ cells using immunofluorescence staining. In the early spermatogenesis, the GB cells generated from an asymmetrical division of GSC proliferates to produce spermatogonia, which then develop into spermatocytes and undergo twice meiosis to become haploid spermatids. The premeiotic germ cells, including GSCs, GBs, and spermatogonia are small. Before meiosis, cells are in the growth and division phase, and after the meiosis S phase, the size increases by about 25 times, dividing from a single spermatogonia to 16 spermatogonia. After two rounds of meiosis, the resulting 64 sperm cells entered the remodeling stage. In this study, we observed that germ cells marked by DNA and Vasa were mainly concentrated at apex of the testis in the control testes (Figure 2A-A''), however, undifferentiated germ cells were accumulated in whole *bamGal4>ValRS-m-hp* testes (Figure 2B-B''). Moreover, cysts of different periods containing varying numbers of germ cells were observed in the control testes (Figure A''), but 32-cell stage cysts were not found in the *ValRS-m* knockdown testes (Figure 2B'').

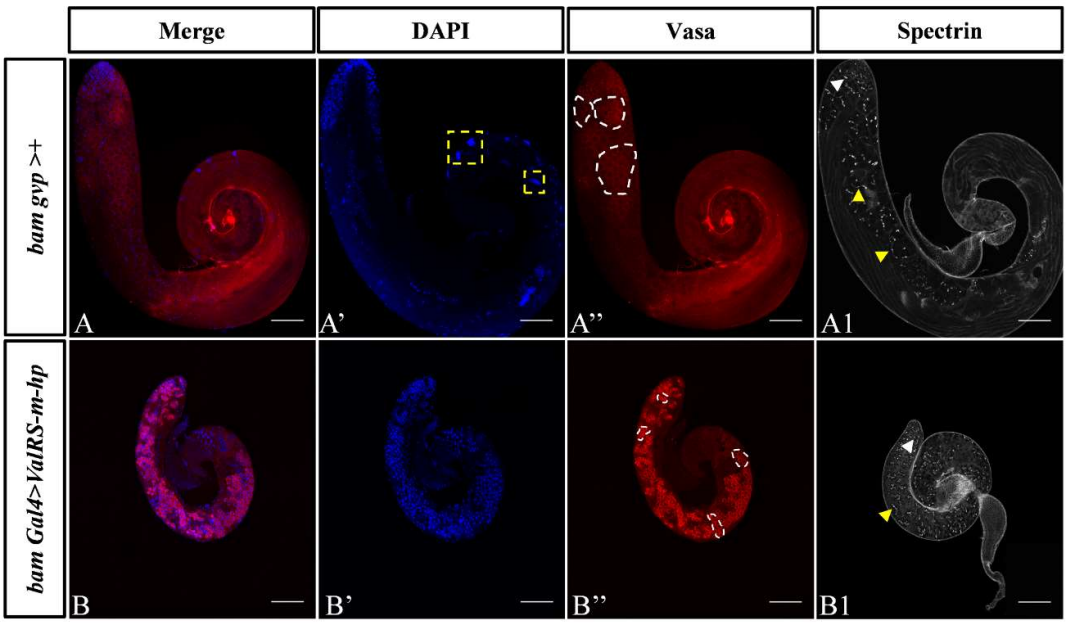

 doi:10.20944/preprints202405.0712.v1

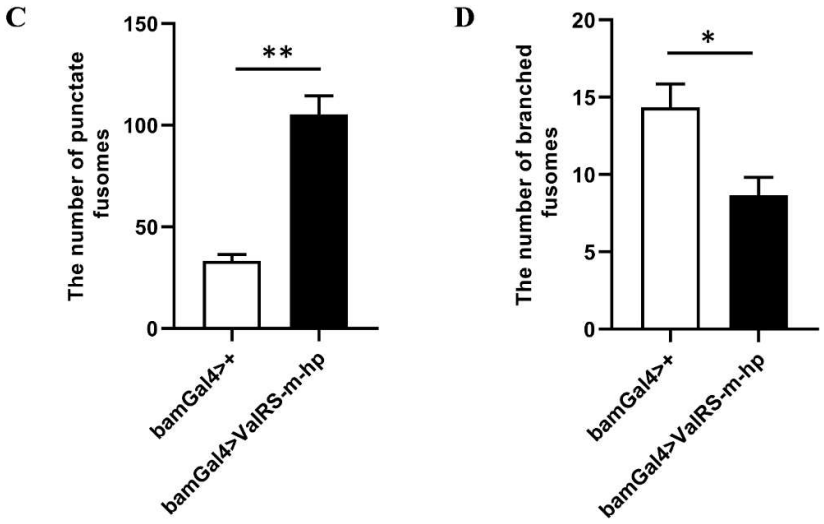

Figure 2. Reduction of *ValRS-m* restrained germline differentiation. (**A-A''**): Immunostaining of Vasa (red) and DAPI (blue) in testes from control *bamGal4*>+ males and *bamGal4>ValRS-m-hp* males. Vasa is a pan-marker for germ cells (**A'', B''**). The yellow boxes represent sperm clusters (**A'**). The white boxes represent germ cell cysts (**A'', B''**). The antibody against α-spectrin labels the fusomes (**A1, B1**), which exhibited two shapes: the round fusomes (indicated by white arrowhead) and branched fusomes (yellow arrowheads). The number of punctate fusomes (**C**) or branched fusomes (**D**) in the control *bamGal4*>+ (n = 10) and *ValRS-m* RNAi (n = 8) testes was quantified. **P*<0.05; ** *P*<0.01. Scale bars,100 μm.

Meanwhile, we found in this study, the fusomes, which are connections and unique structures among germ cells, undergo dynamic changes from a punctate to a branched morphology during germline differentiation germ cells [21,22], have markedly different distribution between *ValRS-m* RNAi and control testes. The number of punctate fusomes increased apparently and the number of branched fusomes decreased in *ValRS-m* RNAi testes compared to control testes (Figure 2A1, B1, C, D). The fusomes branches throughout germ cells differentiation within a cyst, synchronizing the behavior of germ cells [23]. Previous study has illustrated the visualization of dot-like fusomes, also named punctate fusomes, at the apical tip of testes connecting GSCs and their daughter GBs, as well as the branched network that strings spermatogonia or spermatocytes together within a cyst [24]. Therefore, the accumulation of punctate fusomes far from hub cells implies over proliferation or differentiation defects in fly testes. The results demonstrated that downregulation of *ValRS-m* led to germ cell differentiation defects and induced GSC-like cysts.

2.3. Knockdown of ValRS-m Disrupts the Mitochondrial Fusion and ATP Synthesis

Mitochondrial fusion is necessary for normal spermatogenesis in *Drosophila* [25]. Therefore, to further explore the function of *ValRS-m* during germline differentiation, we used mitochondrial Staining (Mito) to label mitochondria, anti-VDAC1/Porin antibody to label the outer mitochondrial membrane for immunofluorescence staining. The results showed that compared with the control testes, the mitochondrial content in the testes after *ValRS-m* knockdown was significantly increased, and most of the locations were concentrated at the end of the testes, indicating a significant increase in cell proliferation (Figure 3A', 3D). Moreover, the VDAC1 morphology in the control testes gradually aggregated from granular to linear. In contrast, in the knockdown testes, only granular and diffuse signals were observed, and no linear mitochondria were found (Figure 3B'). Meanwhile, ATP5A (also named bellwether, blw), as the alpha subunit of the mitochondrial F1F0 ATP synthase complex (complex V), the final enzyme of the oxidative phosphorylation pathway, were significantly weakened in the *ValRS-m* knockdown testes (Figure 3C'). This observation indicated that less *ValRS-m* causes abnormalities in the differentiation of male germ cells by affecting the mitochondria.

 doi:10.20944/preprints202405.0712.v1

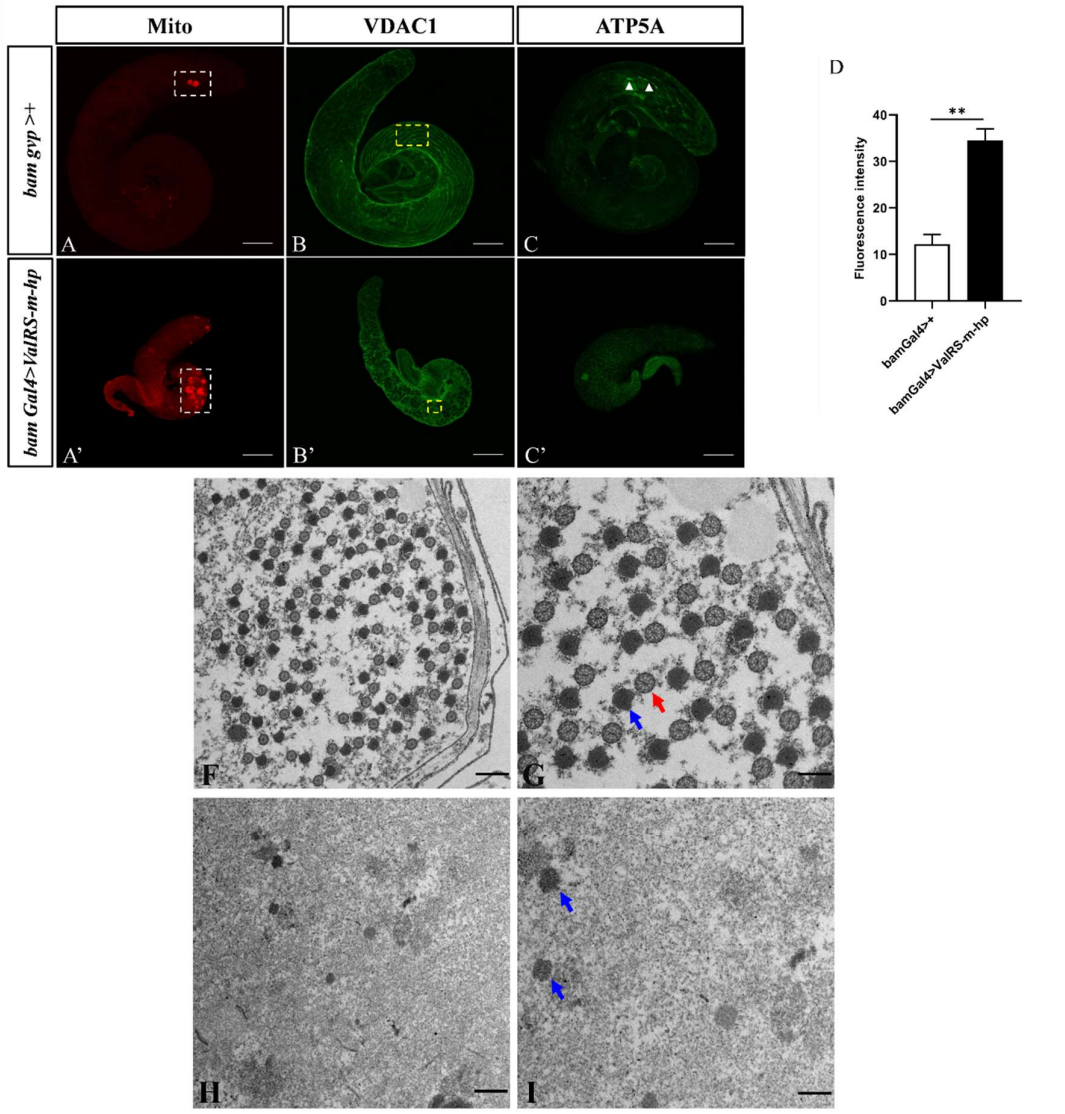

Figure 3. Knockdown of *ValRS-m* affects mitochondrial structure and function in spermatogenesis. (**A-C**): Control testis. (**A'-C'**): ValRS-m knockdown testis. **(B, B')**: White boxes indicate mitochondria (Mitochondrial markers). Yellow boxes indicate mitochondrial envelope morphology (VDAC1 markers). White arrows indicate ATP signaling (ATP5A markers). The mean mitochondrial staining (Mito) signals (n = 8) in testes (**D**). (**F-I**) Transmission electron microscopy (TEM) images showing mitochondrial morphogenesis during spermatogenesis. Pre-individualization spermatids in control testes (**F, G**) show synchronized development of their mitochondrial derivatives in the cysts, where paracrystalline material (blue arrow in **G**) accumulates in the major mitochondrial derivative as a contiguous dense material at the attachment site of the axoneme (red arrow in **I**). A few scattered mitochondrial derivatives existed (blue arrow in **I**) but any axoneme were not seen in the ValRS-m RNAi testes (**H, I**). **G** and **I** represent magnifications of F and H respectively. ** P<0.01. Scale bars, 100 μm (**A-C, A'-C'**); 1 μm (**F, H**); 500 nm (**G, I**).

It is known that the morphology of mitochondria is correlated with their metabolic activity [26]. Inner-mitochondrial-membrane morphology and cristae organization are crucial for the assembly and proper function of the oxidative phosphorylation (OXPHOS) system, responsible for ATP synthesis [27]. Evidences have revealed that abnormal mitochondrial morphology is coupled with the failure of spermatid development, such as Cnt1 and cyt-c1L [28,29]. Additionally, given that *ValRS-m* was located at mitochondria, we used transmission electron microscopy to examine the mitochondrial structure in *ValRS-m* knockdown testes. In control testes, the normal axonemes, containing an ordered '9+2' microtubule structure was observed in early round spermatids. The synchronized development of the major mitochondrial derivatives in the cysts, was gradually deposited with dense paracrystalline material at the attachment site of the axoneme (Figure 3F, 3G). However, the *ValRS-m* knockdown testes lost their synchrony in the cyst and the mitochondrial derivatives became less and loose.

 doi:10.20944/preprints202405.0712.v1

Especially, we could not see any flagellar axoneme that expect to see in elongating spermatid (Figure 3H, 3J). Taking together, our data demonstrated that *ValRS-m* RNAi may inhibit the differentiation of germ cells by affecting the early mitochondrial fusion during early spermatogenesis.

2.4. Knockdown of ValRS-m Leads to Excessive Apoptosis in Testes

Considering the defects in mitochondrial dynamics observed and the stagnation of germ cell differentiation, we speculate that cell death could be induced. Therefore, we thus examined testes using the TUNEL assays. The results showed that the fluorescence signals of TUNEL in *ValRS-m* knockdown testes were significantly stronger (Figure 4B‘’’) than those in the control testes (Figure 4A‘’’). In addition, the TUNEL signal was mainly concentrated in the mid-posterior region, where sperm clusters are supposed to be, in the base of the *ValRS-m* knockdown testes (Figure 4B‘’’). In addition, most apoptotic signals appeared spherical, indicating that apoptosis was likely taking place in the whole cyst of spermatocytes that failed to continue cell differentiation. This demonstrates that *ValRS-m* knockdown leads to excessive apoptosis in fly testes.

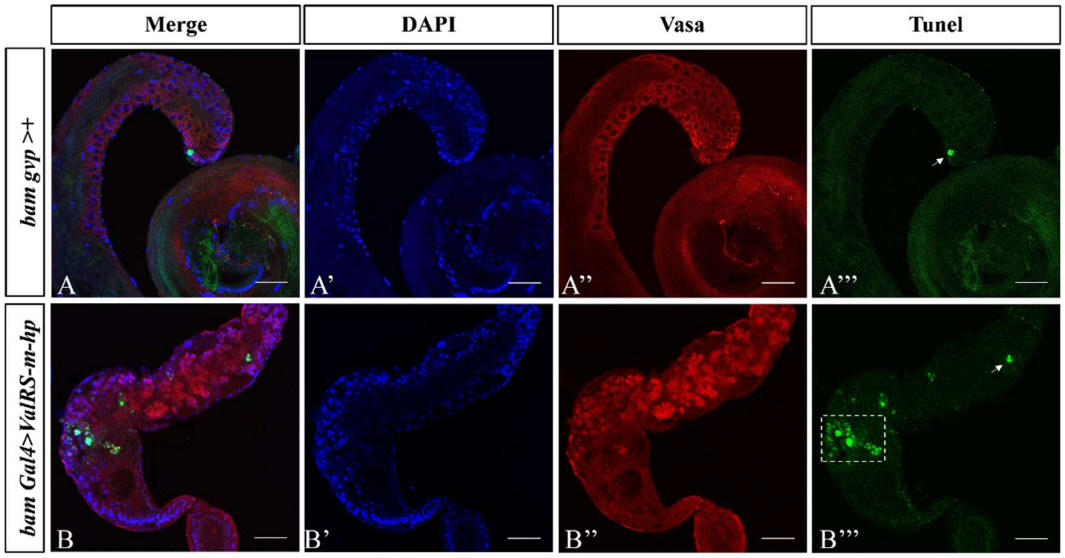

Figure 4. Knockdown of *ValRS-m* induces apoptosis in the testes. (**A**) The Tunel (green) signal at the apical region of the testes from *bamGal4*>+ males (white arrow in **A‘’’**), is not only present at the apical, but more concentrated in the middle and rear segments in the *ValRS-m* knockdown testis (**B**, white box in **B‘’’**). DAPI (blue) stained the nuclei. Vasa (red) stained the germ cells. The single channel images for DAPI staining were shown in (**A’, B’**). The single channel images for Vasa staining were shown in (**A’’, B’’**). The single channel images for Tunel staining were shown in (**A’’’, B’’’**). Scale bars: 50 μm.

2.5. Absence of ValRS-m Alters the Expression Profiles of Genes in Testes

To evaluate the effect of *ValRS-m* on the expression of spermatogenesis-related genes, we performed transcriptomic expression profiling of the testes in response to *ValRS-m* depletion. A total of 17 143 genes were identified through this sequencing. The numbers of expressed genes, total mapped reads and unique matches for each sample are shown in Table S1. A total of 7710 differentially expressed genes (DEGs) were identified in the *ValRS-m*-knockdown testes, including 2985 upregulated and 4725 downregulated DEGs (the absolute value of log2 fold-change >1 and *P* value < 0.05) (Figure 5A). Among DEGs, the down-regulated genes were mainly highly expressed in the testes, and the up-regulated genes were mainly highly expressed in the ovary (Figure 5B), which imply *ValRS-m* play critical role on *Drosophila* reproduction. To further analyze the biological events induced by *ValRS-m* RNAi during spermatogenesis, we performed gene ontology (GO) enrichment analysis for these DEGs according to their functional categorization. The upregulated DEGs were primarily enriched in processes including cytoplasmic translation (87), rRNA processing (63) and cytosolic large ribosomal subunit (49) (Figure 5C), while the downregulated DEGs were enriched in processes such as microtubule-based movement (71), microtubule-associated complex (64), ciliary

 doi:10.20944/preprints202405.0712.v1

part (53) and 46 DEGs were involved in mitochondrial transport (Figure 5D). Moreover, we performed the KEGG pathway analysis for these DEGs. Among the upregulated genes, the top three KEGG pathways with the highest enrichment were ribosome, huntington disease and spliceosome (Figure 5E). Meanwhile, the downregulated DEGs mainly were enriched in glycolysis/gluconeogenesis, glucagon signaling pathway and pyruvate metabolism pathway (Figure 5F).

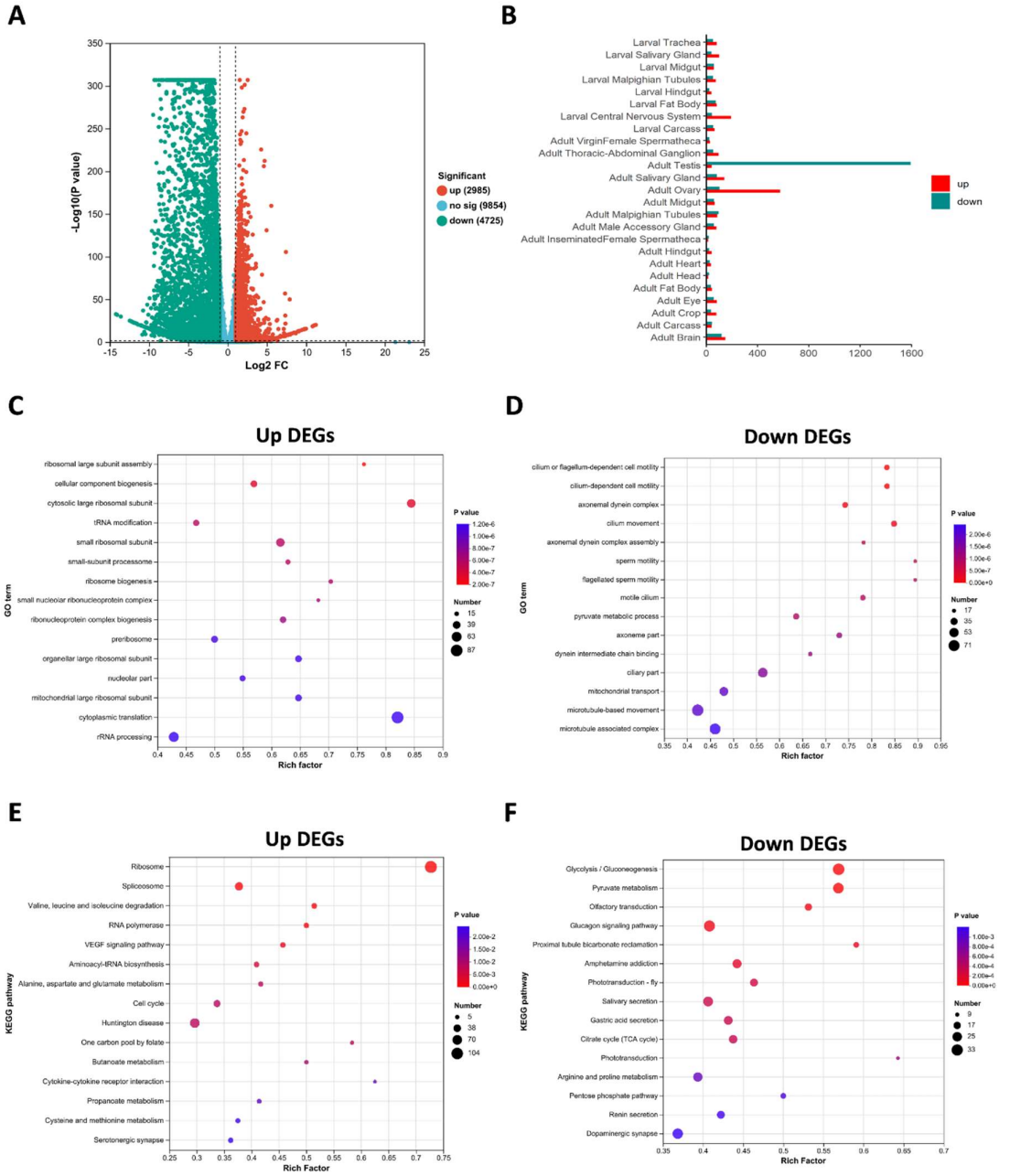

Figure 5. Transcript alterations were assessed by RNA-seq after *ValRS-m* knockdown in testes. (**A**) Volcan plot of differentially expressed genes (DEGs) from comparison of the control and *ValRS-m* knockdown groups. (**B**) Tissue expression profile of differentially expressed genes after *ValRS-m* knockdown in testis. (**C**) GO enrichment analysis of up-regulative DEGs in the testes of *Bam Gal4>ValRS-m-hp* relative to the control. (**D**) GO enrichment analysis of down-regulative DEGs in the testes of *Bam Gal4>ValRS-m-hp* relative to the control. (**E**) KEGG enrichment analysis of up-DEGs in the testes of *ValRS-m* RNAi relative to the control. (**F**) KEGG enrichment analysis of down-DEGs in the testes of *ValRS-m* RNAi relative to the control.

 doi:10.20944/preprints202405.0712.v1

To confirm these effects, further validation of the candidate genes from the transcriptomic data by qRT-PCR is conducted in Table S2. We performed RT-qPCR to detect the expression of 28 DEGs associated with mitochondria between *ValRS-m*-knockdown and control testes (Table 1). In line with the transcriptome results, their expression was significantly decreased in the *ValRS-m* knockdown testes (Figure 6A). Furthermore, according to FlyBase, the DEGs related to maintaining mitochondrial morphology are *mics1*, *Mul1*, and *Knon*. The DEGs related to the mitochondrial electron transport are *UQCR-11L*, *Cyt-c-d*, and *ND-B14.5AL*. Meantime, five genes including *CysRS-m*, *OXA1L*, *VhaM9.7-d*, *Vha100-3*, and *Hsc70-1* are involved in ATPase binding activity and ATP synthase. Additionally, GO analysis indicated that six DEGs involved in the meiotic were all downregulated significantly in *ValRS-m* RNAi testes, supported by the qRT-PCR results (Figure 6B). Among these genes, *Cbc* (*crowded by cid*) is essential for the meiotic, which works together with tRNA splicing endonuclease subunit 54 (*Tsen54*) to regulate the transition to meiosis during spermatogenesis [30]. The other four genes, including *Aly*, *Comr*, *Topi*, and *Wuc* as encoding tMAC (testis-specific meiotic arrest complex) complex members, playing gene activator in spermatogonia that help to activate meiosis [9]. Taken together, the transcriptional profile analysis and qRT-PCR results demonstrated that *ValRS-m* may block the differentiation of sperm cells by destroying the mitochondrial morphology and function, ultimately results in the failure of meiotic and the inability to produce mature sperm in male *Drosophila*.

Table 1. Classification of DEGs that were downregulated (fold change ≥ 2, *P* value < 5%) in *ValRS-m* -knockdown males compared with controls by qRT-PCR.

Annotation ID	Gene Name	Description
Male meiosis-related		
CG2075	*Aly* (always early)	the onset of spermatid differentiation
CG13493	*Comr* (cookie monster)	involved in spermatogenesis and transcription regulation
CG8484	*Topi* (matotopetli)	male meiotic division and spermatid differentiation
CG12442	*Wuc* (Wake-up-call)	male meiotic nuclear division
CG5970	*Cbc* (crowded by cid)	required at the transition to meiosis in spermatogenesis
CG5626	*Tsen54* (tRNA splicing endonuclease subunit 54)	tRNA processing
Mitochondria-related		
CG14128	*Sprn* (Spermitin)	testis-specific mitochondrial lumen protein
CG1287	*mics1* (Mitochondrial morphology and cristae structure 1)	maintenance of mitochondrial morphology
CG11196	*Dic3* (Dicarboxylate carrier 3)	mitochondrial dicarboxylate carrier
CG8330	tomboy40	import of protein precursors into mitochondria
CG6691	*ttm3* (tiny tim 3)	mitochondrial protein translocation
CG12201	*GC2* (Glutamate Carrier 2)	catalyzes the transport of L-glutamate across the inner mitochondrial membrane
CG4706	*mAcon2* (Mitochondrial aconitase 2)	enable 4 irons, 4 sulfur cluster binding activity
CG30354	*UQCR-11L* (Ubiquinol-cytochrome c reductase 11 kDa subunit-like)	mitochondrial electron transport
CG13263	*cyt-c-d* (Cytochrome c distal)	Electron carrier protein, sperm individualization
CG12736	*mEFTu2* (mitochondrial translation elongation factor Tu 2)	bring aminoacyl-tRNA to the ribosome during the elongation phase of mRNA translation
CG14508	*cyt-c1L* (Cytochrome c1-like)	enable ubiquinol-cytochrome-c reductase activity
CG8257	*CysRS-m* (Cysteinyl-tRNA synthetase, mitochondrial)	enable ATP binding activity and cysteine-tRNA ligase activity

 doi:10.20944/preprints202405.0712.v1

CG6404	*OXA1L* (OXA1L mitochondrial inner membrane protein)	mitochondrial proton-transporting ATP synthase complex assembly
CG7311	*Gpo3* (Glycerophosphate oxidase 3)	enable glycerol-3-phosphate dehydrogenase (quinone) activity
CG6412	*mEFTs* (mitochondrial translation elongation factor Ts)	recharge the products of mEFTu1 and mEFTu2 with GTP
CG14290	*Mpc1* (Mitochondrial pyruvate carrier)	transports pyruvate across the mitochondrial inner membrane
CG1134	*Mul1* (Mitochondrial E3 ubiquitin protein ligase 1)	in the control of mitochondrial morphology by promoting mitochondrial fission
CG6914	*ND-B14.5AL* (NADH dehydrogenase (ubiquinone) B14.5 A subunit-like)	mitochondrial electron transport, NADH to ubiquinone
CG5718	*SdhAL* (Succinate dehydrogenase, subunit A (flavoprotein)-like)	mitochondrial respiratory chain complex II
CG7813	*Knon* (knotted onions)	Nebenkern assembly
CG14909	*VhaM9.7-d* (Vacuolar H+ ATPase M9.7 subunit d)	proton-transporting ATPase activity
CG4683	*Tengl4* (Testis EndoG-Like 4)	active in mitochondrial inner membrane and nucleus
CG30329	*Vha100-3* (Vacuolar H+ ATPase 100kD subunit 3)	ATPase binding activity
CG12162	*Poldip2* (Polymerase (DNA-directed), delta interacting protein 2)	active in mitochondrial nucleoid and nucleus
CG7615	*Fig* (fos intronic gene)	active in mitochondrion
CG8937	*Hsc70-1* (Heat shock protein 70 cognate 1)	ATP hydrolysis activity
CG3092	CG3092	protein insertion into mitochondrial inner membrane from matrix
CG31913	CG31913	mitochondrial cytochrome c oxidase assembly

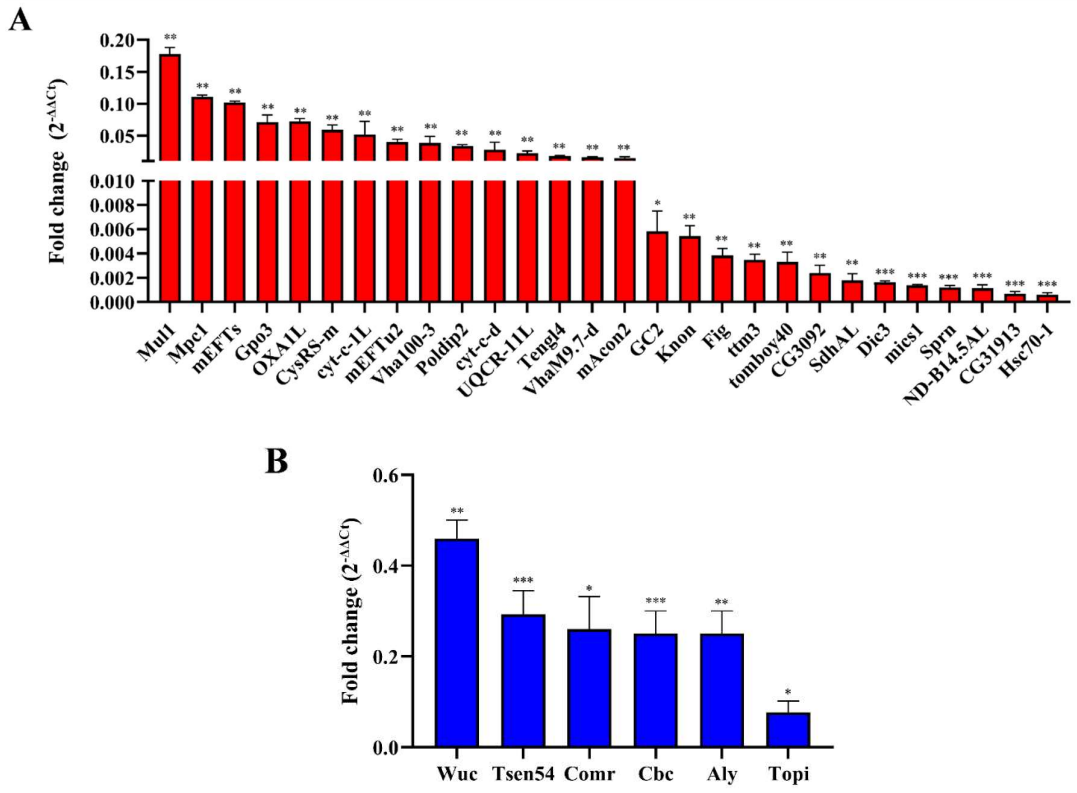

Figure 6. RT-qPCR validation of DEGs after *ValRS-m* knockdown in testes. (**A**) DEGs associated with mitochondria. (**B**) DEGs related to the meiosis. **P* < 0.05; ***P* < 0.01; ****P* < 0.001.

 doi:10.20944/preprints202405.0712.v1

3. Discussion

Spermatogenesis is a complex process of cell differentiation, and the transition of cell state is regulated by a strict cascade [6]. The transition process from spermatogonia to primary spermatocyte is very essential in *Drosophila* spermatogenesis, in which large numbers of genes are involved along with transcriptional and morphological changes, and about 1500 genes are estimated to be expressed only in spermatocytes by genome-wide microarray data [31,32]. In this study, we found that the disappearance of both sperm bundles and mature sperm in the spermatogenesis have been observed in one day old *ValRS-m* RNAi testes, implying the role of *ValRS-m* in regulating spermatogenesis and testes development. Especially, we characterized *ValRS-m* as a crucial factor in regulating the transition from primary spermatocytes to spermatid in the *Drosophila* testes, through immunofluorescence staining of Vasa and Spectrin (Figure 2).

ValRS-m gene is localized in mitochondria, which was the powerhouses of eukaryotic cells due to their ability to produce ATP through oxidative phosphorylation [17,33]. ATP production is essential for sperm motility, capacitation and acrosomal reactions [34]. In somatic cells, as cells enter interphase, mitochondria exhibit an elongated network pattern and aggregate in the nucleus and pericellular. In contrast, during most mitosis, mitochondria exhibit a fragmented network pattern scattered throughout the cytoplasm [35,36]. The development and meiosis of germ cells are much more complex than somatic cells. For example, sperm and eggs undergo meiosis and the complex dynamic distribution of the cytoskeleton. These processes require large amounts of ATP to maintain [37,38]. In this study, we found that ATP signaling was very powerful in control testes and highly expressed in both round and elongated spermatids. However, ATP5A signaling was almost undetectable in *ValRS-m* knocked-down testes (Figure 3). Therefore, these results suggest that *ValRS-m* knockdown leads to the obstruction of ATP synthesis in testes.

Studies have shown that mitochondria can participate in a series of activities in sperm formation, including the fusion and aggregation of early active mitochondria to form a nebenkern [39]. Dorogova et al (2013) showed that the primary spermatocytes of wild-type *Drosophila* underwent a pre-meiosis growth phase, and the number of mitochondria increased significantly, the mitochondria of mature spermatocytes are compact and evenly distributed in the cytoplasm [40]. Through transmission electron microscopy, we speculated that the spermatogenesis of *ValRS-m* knock-down testes may be stagnant in the primary spermatocyte stage without subsequent meiosis, because the axial and fibrous complex is missing and the nucleus is in a diffuse state in the absence of *ValRS-m*.

This prediction was further confirmed by subsequent RNA-seq and qRT-PCR results. The RNA-seq analysis and qRT-PCR revealed that many meiosis-related genes were significantly decreased in *ValRS-m* RNAi testes compared to the control testes including *Cbc* and *Tsen54* (Figure 6B). The expression of *Cbc* gene encodes a polynucleotide 5'-hydroxyl-kinase required at the transition to meiosis in spermatogenesis, as well as the expression of *Tsen54* is conducive to the transition to meiosis [30]. At the same time, the tMAC complex helps to activate meiosis of spermatocytes [41]. QRT-PCR results also showed that these tMAC complex encoding genes, including *Aly*, *Comr*, *Topi*, and *Wuc* expression level were down-regulated significantly in the lack of *ValRS-m*. Due to *Aly*, *Comr* and *Topi* are only expressed in primary spermatocytes [10,32,41], implying that the meiosis is suppressed on account of knockdown of *ValRS-m* through inhibiting the transcription of these meiosis related genes in the primary spermatocyte, hence resulting in the stalling of spermatogenesis. Moreover, these spermatocytes that did not enter meiosis eventually underwent apoptosis, which is consistent with the increase of apoptotic signal tunnel observed (Figure 4).

Furthermore, we found that *ValRS-m* RNAi interrupts the expression of multiple mitochondrial genes (Figure 6A). These mitochondrial genes play a critical role in mitochondrial function and spermatogenesis. For example, Cyt-c1, as a subunit of mitochondrial respiratory chain complex III, is involved in oxidative phosphorylation mediating electron transport from cytochrome b to cytochrome c [42,43]. *Sprn* is specifically located in the mitochondrial nebenskern, playing a role in sperm elongation [44]. *Mics1* encodes mitochondrial intima proteins and interacts with proteins encoded by *chchd2* to enhance oxidative phosphorylation [45]. Studies have shown that Knon, an unusually large paralogic homologue of the ATP synthase subunit d, participates in the internal shaping of the nebenskern forming mitochondrial membrane during spermatogenesis in *Drosophila*. Male flies lacking *knon* are sterile [46]. *Cyt-c1L* encodes a subunit of mitochondrial respiratory chain complex III, involved in mitochondrial ATP synthesis and coupled proton transport process. We

 doi:10.20944/preprints202405.0712.v1

previously found that the knockdown of *Cyt-c1L* could result in abnormal axial filament, unable to form individual complex, and lead to abnormal spermatocyte apoptosis and immature sperm, resulting in male infertility [29]. Taken together, these studies explore that the deficiency of *ValRS-m* might inhibit spermatogenesis by affecting mitochondrial structure and function in flies.

The effect of *ValRS-m* RNAi on *Drosophila* spermatogenesis is extensive and significant. To further reveal its regulatory mechanism on male fly fertility, we have identified 7710 DEGs in *ValRS-m* RNAi testes by RNA-Seq, including 4725 down-regulated genes and 2985 up-regulated genes. We found that the metabolic pathways associated with up-regulated DEGs were most involved in the ribosome pathway (104 genes), such as RPS3 (Ribosomal protein S3), RPL22 (Ribosomal protein L22), RPL36 (Ribosomal protein L36), etc. Studies have shown that most ribosomal proteins not only play a role in the biological reaction process of ribosomes and protein synthesis, but also affect the process of biological somatic activities by performing "extra-ribosomal" functions, which are involved in many biological processes, including growth and development, cell apoptosis and aging processes [47]. The fruit fly ribosome contains 79 different proteins, among which RPS3 is not only involved in translation and ribosome maturation, but also can recognize DNA damage [48]. Importantly, RpS3 plays a critical role in regulating spermatid elongation and individualization [49]. In addition, the deletion of *RpL22* gene is also common in many types of cancer and cell lines [50], and *RPL36* knock-down results in a reduced number of germ cells in the testes and few or no mature sperm in the seminal vesicles [51].

Additionally, the down-regulated DEGs is most enriched in glycolysis/gluconeogenesis pathway and pyruvate metabolic pathway, and is also involved in citric acid cycle and pentose phosphate metabolic pathway, which are all carbohydrate metabolic pathways. Glycolysis is a vital component of semen activity because it is involved in capacitation, provides a second energy source for spermatocyte development. It is closely associated with sperm functional maturation and epididymal transport [52]. Studies have shown that carbohydrate metabolism is closely related to spermatogenesis [53,54]. For example, the testicles promote carbohydrate metabolism in adjacent gut sites through JAK-STAT signaling in fruit flies [10,55]. The male intestine secretes citrate to the adjacent sperms, thus promoting sperm maturation [53]. We found that *ValRS-m* knockdown significantly inhibited the expression level of genes involved in carbohydrate synthesis, thus it may have an impact on the energy required for spermatogenesis. Therefore, it is speculated that the knockdown of *ValRS-m* may affect the function of various ribosomal proteins and carbohydrate metabolism hence destroy the spermatogenesis.

4. Materials and Methods

4.1. Fly Stocks

Flies were reared on a standard cornmeal/yeast diet at 25°C and under non-crowded conditions (200 ± 10 eggs per 50-ml vial of media in the 150 ml conical flask). Transgenic *ValRS-m*-hp *D. melanogaster* line was obtained from the Tsinghua Fly Center (Beijing). The *bamGal4 vp16* line was a kind gift from Professor Zhaohui Wang at the Institute of Genetics and Developmental Biology, Chinese Academy of Sciences. All flies were raised in the 150 mL conical flasks with standard corn/sugar medium at 25°C.

4.2. Fertility Test

Gene knockdown flies (*bamGal4>ValRS-m-hp*) were generated by crossing transgenic RNAi males with virgin *bamGal4* females. Flies from the cross between w1118 males and *bamGal4* females were used as the control (*bamGal4>+*). The 1-day-old gene knockdown males were crossed with 3-4-day-old w1118 females to assay male fertility. For each biological repeat, 15 males and 10 females were used. After 12 h of crossing, males were removed, and then eggs were collected and incubated at 25°C for 24 h. Hatch rates were determined from the proportion of hatched eggs to total eggs. Three biological repeats per cross type were performed.

4.3. Immunofluorescence Staining

One-day-old fly testes were dissected in PBS, fixed for 30 min in 4% paraformaldehyde at room temperature, and washed in wash buffer [phosphate buffered saline (PBS)/0.1% Triton X-100] three

 doi:10.20944/preprints202405.0712.v1

times for 15 min each. The testis samples were blocked for 30 min in 5% normal goat serum, incubated overnight at 4°C with primary antibodies. Primary antibodies were used at the following dilutions: rabbit anti-Vasa (1:100, cat. no. AB760351, Developmental Studies Hybridoma Bank, Iowa, IA, USA), mouse anti-spectrin (1:100, cat.no. AB528473, Developmental Studies Hybridoma Bank), anti-ATP5A. Secondary antibodies were used at the following dilutions: phalloidin (1:200, cat. no. BMD00084, Abbkine), rabbit 594 and mouse 488 (1:200, cat. no. A23420 and A23210, Abbkine). All samples were mounted on a glass slide with 4′-6-diamidino-2-phenylindole (DAPI) (2 μg ml−1, cat. no. S2110, Solarbio, Beijing, China) solution [56]. Fluorescence images were collected using a Leica SP8 laser confocal microscope (Leica, Germany).

4.4. Transmission Electron Microscopy

The testes were dissected from 1d *bamGal4*/*ValRS-m-hp* and *bamGal4*>+ males in PBS, and fixed in 2.5% glutaraldehyde (0.2 M phosphate buffer, pH 7.4) at 4°C overnight. Then these testes were washed in phosphate buffer and post-fixed in 1% OsO4 for one hour. After double fixation, the samples were dehydrated through an ascending series of ethanol (30%, 50%, 70%, 80%, 100%, ten minutes for each concentration and doubled for 100%, and then embedded in Araldite (EMbed 812, China). Ultrathin sections (80 nm) were obtained in Leica Ultracut 7. The sections were placed on copper grids, stained with 2% uranyl acetate for 15 min, rinsed twice with H2O for five minutes, then stained with lead citrate for 15 min. The stained samples were observed using H-8100 transmission electron microscope (Hitachi, Tokyo, Japan) operating at 100 kV.

4.5. TUNEL Staining

TUNEL staining (TdT-mediated dUTP nick end labeling) was performed as follows in this study. Thirty pairs of 1-day-old *Drosophila* testis were dissected and fixed in 4% paraformaldehyde solution at RT for 40 min, then washed four times (15 minutes each time) in PBST (phosphate buffer, PBS + 0.1% Triton X-100). The sample was then incubated with the TUNEL reaction mixture (5 μl TdT enzyme solution and 45 μl fluorescein-dUTP tag solution) in a dark environment at 37°C for three hours (Roche, Germany). After rinsing three times with PBST in the dark, the testes used an anti-fading medium (Solarbio, Beijing, China) containing 2 μg/ml DAPI to fix on the glass slide. The Leica SP5 laser confocal microscope was used to observe and take photos.

4.6. RNA Extraction, Library Preparation and Sequencing

To screen the genes related to *ValRS-m* during spermatogenesis, we collected 80-100 testes samples from *bamGal4*/*ValRS-m-hp* and *bamGal4*>+ males. These testes were used for transcriptomic analysis. Six cDNA libraries were constructed and sequenced on the Illumina Novaseq 6000 platform (San Diego, USA) following the standard protocols set by Majorbio Bio-Pharm Technology Co. Ltd. (Shanghai, China). Subsequently, clean reads were mapped to the genome of *Drosophila* melanogaster (Flybase, dmelr6.15 genome) using TopHat (http:// tophat. cbcb.umd. edu/) software. After assembly of the mapped reads, the unigenes were run against a non-redundant database.

To identify DEGs (differential expression genes) between two different groups, the expression level of each gene was calculated according to the transcripts per million reads (TPM) method. RSEM (http://deweylab.biostat.wisc.edu/rsem/) was used to quantify gene abundances [57]. DEGs were determined with a cutoff of |log2 fold change (RNAi/control) |≥ 1 and p-value ≤ 0.05, as the criteria used in the previous study [58]. In addition, functional-enrichment analysis including GO (Gene Ontology, http://www.geneontology.org) and KEGG (Kyoto Encyclopedia of Genes and Genomes, http://www.genome.jp/kegg/) were performed to identify which DEGs were significantly enriched in GO terms and metabolic pathways at P value≤0.05 compared with the whole-transcriptome background. GO functional enrichment and KEGG pathway analysis were carried out by Goatools and KOBAS [59].

4.7. Quantitative Real-Time PCR

The assay was performed as previously described [18]. Total RNA was extracted using Trizol (cat. no. 15596026, Invitrogen, Waltham, MA, USA) from testes and ovaries of 1-day- old adult w1118, as well as testes from bamGal4/ValRS-m-hp and bamGal4>+ males. First-strand cDNA was synthesized from 2 μg of total RNA using EasyScript first-strand cDNA synthesis SuperMix Kit (cat.

 doi:10.20944/preprints202405.0712.v1

no. AT321-01, TransGen Biotech, Beijing, China). qPCR was performed with specific primers (Table S2) using a Miniopticon system (Bio-Rad, Hercules, CA, USA) with a Platinum SYBR Green qPCR SuperMix (cat. no. Q711-02, Vazyme, Shanghai, China) as described previously (Zheng et al., 2018). The qPCR cycling programmed was as follows: 95°C for 3 min, followed by 40 cycles of 95°C for 10 s, 55–60°C (depending on different primers) for 30 s and 65°C for 5 s. Then, a melting curve was constructed from 55°C to 98°C. The relative expression of the gene was calibrated against the reference gene *rp49* using the 2−ΔΔCT calculation method: $\Delta\Delta Ct=(Ct_{Target}-Ct_{rp49})$*ValRS-m* RNAi−$(Ct_{Target}-Ct_{rp49})$control [60].

4.8. Statistical Analysis

Statistical analysis was performed using GraphPad Prism software (GraphPad Inc., La Jolla, CA, USA). Student's test was used for two-group comparisons. A value of $P< 0.05$ was considered significantly different. The statistical details were indicated in the corresponding figure legends.

5. Conclusions

In conclusion, our study demonstrates that *ValRS-m* is crucial for meiosis of spermatocyte and spermatid mitochondrial morphology in *Drosophila*. The most striking finding was a significant reduction in meiosis-related genes and multiple mitochondrial-related genes, determining whether spermatocytes can differentiate smoothly into sperm clusters and mature sperm. Our findings provide a rich resource to understand the mechanisms of spermatogenesis especially in male germ cells differentiation. Further investigations should examine the relationships between *ValRS-m* and these DEGs.

Supplementary Materials: The following supporting information can be downloaded at the website of this paper posted on Preprints.org.

Author Contributions: Funding acquisition, Ya Zheng, Zhi-Xian Cao; Methodology, Xin Duan and Hao Wang; Resources, Yu-Feng Wang; Software, Na Su. All authors have read and agreed to the published version of the manuscript.

Funding: This work was supported by the National Natural Science Foundation of China (no. 31970471) to Y-Z. Opinions, findings, conclusions, or recommendations expressed in this material are those of the authors(s) and do not necessarily reflect the views of the National Natural Science Foundation of China.

Institutional Review Board Statement: Not applicable.

Informed Consent Statement: Not applicable.

Data Availability Statement: The raw sequence data are available at the National Center for Biotechnology Information Short Read Archive database (http://www.ncbi.nlm.nih.gov/sra/) under the accession number PRJNA1108791.All other data are available in this text and Supplementary Files.

Acknowledgments: We thank Professor Zhaohui Wang (Institute of Genetics and Developmental Biology, CAS) for providing *BamGal4* flies.We are grateful to Bi-Chao Xu of the Core Facility and Technical Support, Wuhan Institute of Virology, for her technical support in ultrathin sections and micrography for TEM.

Conflicts of Interest: The authors declare no conflict of interest.

References

1. Sucato, A.; Buttà, M.; Bosco, L.; Di, Gregorio. L.; Perino, A.; Capra, G. Human Papillomavirus and Male Infertility: What Do We Know? *Int J Mol Sci* **2023**, *24*,17562.
2. Fabian, L.; Brill J.A. *Drosophila spermiogenesis*: Big things come from little packages. *Spermatogenesis* **2012**, *2*, 197-212.
3. Chen, H.; Ren, S.; Clish, C.; Jain, M.; Mootha, V.; McCaffery, J.M.; Chan, D.C. Titration of mitochondrial fusion rescues Mff-deficient cardiomyopathy. *J Cell Biol* **2015**, *211*, 795-805.
4. Demarco, R.S.; Eikenes, Å.H.; Haglund, K.; Jones, D.L. Investigating spermatogenesis in *Drosophila melanogaster*. *Methods* **2014**, *68*, 218-227.
5. Yu, J.; Zheng, Q.; Li, Z.; Wu, Y.; Fu, Y.; Wu, X.; Lin, D.; Shen, C.; Zheng, B.; Sun, F. CG6015 controls spermatogonia transit-amplifying divisions by epidermal growth factor receptor signaling in *Drosophila* testes. *Cell Death Dis* **2021**, *12*, 491.
6. Lim, C.; Tarayrah, L.; Chen, X. Transcriptional regulation during *Drosophila* spermatogenesis. *Spermatogenesis* **2012**, *2*, 158-166.

 doi:10.20944/preprints202405.0712.v1

7. Shi, Z.; Lim, C.; Tran, V.; Cui, K.; Zhao, K.; Chen, X. Single-cyst transcriptome analysis of *Drosophila* male germline stem cell lineage. *Development* **2020**, *147*, dev184259.
8. Trost, M.; Blattner, A.C.; Leo, S.; Lehner, C.F. *Drosophila dany* is essential for transcriptional control and nuclear architecture in spermatocytes. *Development* **2016**,*143*, 2664-2676.
9. Laktionov, P. P., Maksimov, D. A., Romanov, S. E., Antoshina, P. A., Posukh, O. V., White-Cooper, H., Koryakov, D. E., & Belyakin, S. N. Genome-wide analysis of gene regulation mechanisms during *Drosophila* spermatogenesis. *Epigenet & chromatin* **2018**,*11*, 14.
10. White-Cooper, H. Molecular mechanisms of gene regulation during *Drosophila* spermatogenesis. *Reproduction* **2010**, *139*, 11–21.
11. Li, A. Y. Z.; Di, Y.; Rathore, S.; Chiang, A. C.; Jezek, J.; Ma, H. Milton assembles large mitochondrial clusters, mitoballs, to sustain spermatogenesis. *Proc Natl Acad Sci U S A* **2023**, *120*, e2306073120.
12. St John, J. C.; Facucho-Oliveira, J.; Jiang, Y.; Kelly, R.; Salah, R. Mitochondrial DNA transmission, replication and inheritance: a journey from the gamete through the embryo and into offspring and embryonic stem cells. *Hum Reprod Update* **2010**, *16*, 488-509.
13. Hales, K. G.; Fuller, M. T. Developmentally regulated mitochondrial fusion mediated by a conserved, novel, predicted GTPase. *Cell* **1997**, *90*, 121-129.
14. Pereira, S.; Adrião, M.; Sampaio, M.; Basto, MA.; Rodrigues, E.; Vilarinho, L.; Teles, EL.; Alonso I.; Leão M. Mitochondrial Encephalopathy: First Portuguese Report of a VARS2 Causative Variant. *JIMD reports* **2018**, *42*, 113-119.
15. Alsemari, A.; Al-Younes, B.; Goljan, E.; Jaroudi, D.; BinHumaid, F.; Meyer, B.F.; Arold, S.T.; Monies, D. Correction to: Recessive *VARS2* mutation underlies a novel syndrome with epilepsy, mental retardation, short stature, growth hormone deficiency, and hypogonadism. *Hum Genomics* **2017**, *11*, 33.
16. Ruzman, L.; Kolic, I.; Radic Nisevic, J.; Ruzic Barsic, A.; Skarpa Prpic, I.; Prpic, I. A novel VARS2 gene variant in a patient with epileptic encephalopathy. *Upsala J Med Sci* **2019**, *124*, 273–277.
17. Begliuomini, C.; Magli, G.; Di Rocco, M.; Santorelli, F. M.; Cassandrini, D.; Nesti, C.; Deodato, F.; Diodato, D.; Casellato, S.; Simula, D. M.; Dessì, V.; Eusebi, A.; Carta, A.; Sotgiu, S. VARS2-linked mitochondrial encephalopathy: two case reports enlarging the clinical phenotype. *BMC Medical Genetics* **2019**, *20*,77-93.
18. Zheng, Y.; Bi, J.; Hou, M.Y.; Shen, W.; Zhang. W.; Ai, H.; Yu, X.Q.; Wang, Y.F. *Ocnus* is essential for male germ cell development in *Drosophila melanogaster*. *Insect Mol Biol* **2018**, *27*, 545-555.
19. Carbonell, A.; Pérez-Montero, S.; Climent-Cantó, P.; Reina, O.; Azorín, F. The Germline Linker Histone dBigH1 and the Translational Regulator Bam Form a Repressor Loop Essential for Male Germ Stem Cell Differentiation. *Cell reports* **2017**, *21*, 3178–3189.
20. Yu, J.; Yan, Y.; Luan, X.; Qiao, C.; Liu, Y.; Zhao, D.; Xie, B.; Zheng, Q.; Wang, M.; Chen, W.; et al. Srlp is crucial for the self-renewal and differentiation of germline stem cells via RpL6 signals in *Drosophila* testes. *Cell Death Dis* **2019**, *10*, 294.
21. Chen, W. Y.; Yan, Y. D.; Luan, X. J.; Wang, M.; Fang, J. Functional analysis of CG8005 gene in *Drosophila* testis. *Hereditas* **2020**, *42*, 1122–1132.
22. Wang, M.; Chen, X.; Wu, Y.; Zheng, Q.; Chen, W.; Yan, Y.; Luan, X.; Shen, C.; Fang, J.; Zheng, B.; Yu, J. RpS13 controls the homeostasis of germline stem cell niche through Rho1-mediated signals in the *Drosophila* testis. *Cell proliferat* **2020**, *53*, e12899.
23. Eikenes, A. H.; Brech, A.; Stenmark, H.; Haglund, K. Spatiotemporal control of Cindr at ring canals during incomplete cytokinesis in the *Drosophila* male germline. *Dev. Biol* **2013**, *377*, 9–20.
24. Jiang, L.; Li, T.; Zhang, X.; Zhang, B.; Yu, C.; Li, Y.; Fan, S.; Jiang, X.; Khan, T.; Hao, Q.; et al. RPL10L Is required for male meiotic division by compensating for RPL10 during meiotic sex chromosome inactivation in mice. *Curr. Biol* **2017**, *27*, 1498–1505.
25. Demarco, R.S.; Jones, D. L. Mitochondrial fission regulates germ cell differentiation by suppressing ROS-mediated activation of Epidermal Growth Factor Signaling in the *Drosophila* larval testis. *Scientific reports* **2019**, *9*, 19695.
26. Joubert, F.; Puff, N. Mitochondrial Cristae Architecture and Functions: Lessons from Minimal Model Systems. *Membranes* **2021**, *11*, 465.
27. Cogliati, S.; Frezza, C.; Soriano, M. E.; Varanita, T.; Quintana-Cabrera, R.; Corrado, M.; Cipolat, S.; Costa, V.; Casarin, A.; Gomes, L.C.; Perales-Clemente, E.; Salviati, L.; Fernandez-Silva, P.; Enriquez, J. A.; Scorrano, L. Mitochondrial cristae shape determines respiratory chain supercomplexes assembly and respiratory efficiency. *Cell* **2013**, *155*, 160-171.
28. Maaroufi, H. O.; Pauchova, L.; Lin, Y. H.; Wu, B. C.; Rouhova, L.; Kucerova, L.; Vieira, L. C.; Renner, M.; Sehadova, H.; Hradilova, M.; Zurovec, M. Mutation in *Drosophila* concentrative nucleoside transporter 1 alters spermatid maturation and mating behavior. Front. Cell Dev. Biol. **2022**, *10*, 945572.
29. Chen, M. Y.; Duan, X.; Wang, Q.; Ran, M. J.; Ai, H.; Zheng, Y.; Wang, Y. F. Cytochrome c1-like is required for mitochondrial morphogenesis and individualization during spermatogenesis in *Drosophila melanogaster*. *J Exp Biol* **2023**, *226*, jeb245277.

 doi:10.20944/preprints202405.0712.v1

30. Wu, J.; Li, X.; Gao, Z.; Pang, L.; Liu, X.; Huang, X.; Wang, Y.; Wang, Z. RNA kinase CLP1/Cbc regulates meiosis initiation in spermatogenesis. *Hum mol genet.* **2021**, *30*, 1569-1578.
31. Parisi, M.; Nuttall, R.; Edwards, P.; Minor, J.; Naiman, D.; Lü, J.; Doctolero, M.; Vainer, M.; Chan, C.; Malley, J.; Eastman, S.; Oliver, B. A survey of ovary-, testis-, and soma-biased gene expression in *Drosophila melanogaster* adults. *Genome biol* **2004**, *5*, R40.
32. Chen, X.; Lu, C.; Morillo Prado, J. R.; Eun, S. H.; Fuller, M. T. Sequential changes at differentiation gene promoters as they become active in a stem cell lineage. *Development* **2011**, *138*, 2441-2450.
33. Li, X.; Fang, P.; Mai, J.; Choi, E.T.; Wang, H.; Yang, X.F. Targeting mitochondrial reactive oxygen species as novel therapy for inflammatory diseases and cancers. *J. Hematol. Oncol* **2013**, *6*, 19.
34. Costa, J.; Braga, P. C.; Rebelo, I.; Oliveira, P. F.; Alves, M. G. Mitochondria Quality Control and Male Fertility. *Biology* **2023**,*12*, 827.
35. Horbay, R., Bilyy, R. Mitochondrial dynamics during cell cycling. *Apoptosis* **2016**, *21*, 1327–1335
36. Madan, S.; Uttekar, B.; Chowdhary, S.; Rikhy, R. Mitochondria lead the way: mitochondrial dynamics and function in cellular movements in development and disease. *Front Cell Dev Biol* **2021**, *9*, 781933
37. Al-Zubaidi, U.; Liu, J.; Cinar, O.; Robker, R. L.; Adhikari, D.; Carroll, J. The spatio-temporal dynamics of mitochondrial membrane potential during oocyte maturation. *Mol Hum Reprod* **2019**, *25*, 695–705.
38. Fleck, D.; Kenzler, L.; Mundt, N.; Strauch, M.; Uesaka, N.; Moosmann, R.; Bruentgens, F.; Missel, A.; Mayerhofer, A.; Merhof, D.; Spehr, J.; Spehr, M. ATP activation of peritubular cells drives testicular sperm transport. *Elife* **2021**,*10*, e62885
39. Detmer, S. A.; Chan, D. C. Functions and dysfunctions of mitochondrial dynamics. *Nat Rev Mol Cell Bio* **2007**, *8*, 870-879.
40. Dorogova, N. V.; Bolobolova, E. U.; Akhmetova, K. A.; Fedorova, S. A. *Drosophila* male-sterile mutation emmenthal specifically affects the mitochondrial morphogenesis. *Protoplasma* **2013**, *250*, 515-520.
41. Beall, E. L.; Lewis, P. W.; Bell, M.; Rocha, M.; Jones, D. L.; Botchan, M. R. Discovery of tMAC: a *Drosophila* testis-specific meiotic arrest complex paralogous to Myb-Muv B. *Genes Dev* **2007**, *21*, 904-919.
42. Chishiki, M.; Takagi, K.; Sato, A.; Miki, Y.; Yamamoto, Y.; Ebata, A.; Shibahara, Y.; Watanabe, M.; Ishida, T.; Sasano, H.; Suzuki, T. *Cytochrome c1* in ductal carcinoma in situ of breast associated with proliferation and comedo necrosis. *Cancer Sci* **2017**, *108*, 1510-1519.
43. Crofts, A.R. The *cytochrome bc1* complex: function in the context of structure. *Annu Rev Physiol* **2004**, *66*, 689-733.
44. Chen, J.V.; Megraw, T. L. Spermitin: a novel mitochondrial protein in *Drosophila* spermatids. *PLoS One* **2014**, *9*, e108802.
45. Meng, H., Yamashita, C., Shiba-Fukushima, K., Inoshita, T., Funayama, M., Sato, S., Hatta, T., Natsume, T., Umitsu, M., Takagi, J., Imai, Y., & Hattori, N. Loss of Parkinson's disease-associated protein CHCHD2 affects mitochondrial crista structure and destabilizes *cytochrome c*. *Nat. Commun* **2017**, *8*, 15500-15518.
46. Sawyer, E. M.; Brunner, E. C.; Hwang, Y.; Ivey, L. E.; Brown, O.; Bannon, M.; Akrobetu, D.; Sheaffer, K. E.; Morgan, O.; Field, C. O.; Suresh, N.; Gordon, M. G.; Gunnell, E. T.; Regruto, L. A.; Wood, C. G.; Fuller, M. T.; Hales, K. G. Testis-specific ATP synthase peripheral stalk subunits required for tissue-specific mitochondrial morphogenesis in *Drosophila*. *BMC Cell Bio* **2017**, *18*, 16-31.
47. Bhavsar, R.B.; Makley, L.N.; Tsonis, P. A. The other lives of ribosomal proteins. *Hum Genomics* **2010**, *4*, 327-344.
48. Yadavilli, S.; Hegde, V.; Deutsch, W. A. Translocation of human ribosomal protein S3 to sites of DNA damage is dependant on ERK-mediated phosphorylation following genotoxic stress. *DNA Repair* **2007**, *6*, 1453-1462.
49. Fang, Y.; Zhang, F.; Zhan, Y.; Lu, M.; Xu, D.; Wang, J.; Li, Q.; Zhao, L.; Su, Y. *RpS3* Is Required for Spermatogenesis of *Drosophila melanogaster*. *Cells* **2023**, 12, 573.
50. Ajore, R.; Raiser, D.; McConkey, M.; Jöud, M.; Boidol, B.; Mar, B.; Saksena, G.; Weinstock, D. M.; Armstrong, S.; Ellis, S. R.; Ebert, B. L.; Nilsson, B. Deletion of ribosomal protein genes is a common vulnerability in human cancer, especially in concert with TP53 mutations. *EMBO Mol*. **2017**, *9*, 498-507.
51. Fang, Y.; Zong, Q.; He, Z.; Liu, C.; Wang, Y. F. Knockdown of *RpL36* in testes impairs spermatogenesis in *Drosophila melanogaster*. *J Exp Zool* **2021**, *336*, 417-430.
52. Storey, B.T. Mammalian sperm metabolism: oxygen and sugar, friend and foe. *Int J Dev Biol* **2008**, *52*, 427-437.
53. Hudry, B.; de Goeij, E.; Mineo, A.; Gaspar, P.; Hadjieconomou, D.; Studd, C.; Mokochinski, J. B.; Kramer, H. B.; Plaçais, P. Y.; Preat, T.; Miguel-Aliaga, I. Sex Differences in Intestinal Carbohydrate Metabolism Promote Food Intake and Sperm Maturation. *Cell* **2019**, *178*, 901-918.
54. Di Giorgio, M. L.; Morciano, P.; Bucciarelli, E.; Porrazzo, A.; Cipressa, F.; Saraniero, S.; Manzi, D.; Rong, Y. S.; Cenci, G. The *Drosophila* Citrate Lyase Is Required for Cell Division during Spermatogenesis. *Cells* **2020**, *9*, 206-218.
55. Greenspan, L. J.; de Cuevas, M.; Matunis, E. Genetics of gonadal stem cell renewal. *Annu. Rev. Cell Dev. Biol* **2015**, *31*, 291-315.

 doi:10.20944/preprints202405.0712.v1

56. Yang, X.; Liu, X.; Li, Y.; Huang, Q.; He,W.; Zhang, R.; Feng, Q.; Benayahu, D. The negative effect of silica nanoparticles on adipogenic differentiation of human mesenchymal stem cells. *Int. J. Mol. Sci* **2017**, *81*, 341.
57. Li, B.; Dewey, C. N. RSEM: accurate transcript quantification from RNA-Seq data with or without a reference genome. *BMC Bioinformatics* **2011**, *12*, 323.
58. Xu, J.; Du, R.; Wang, Y.; Chen, J. RNA-sequencing reveals the involvement of sesquiterpene biosynthesis genes and transcription factors during an early response to mechanical wounding of *Aquilaria sinensis*. *Genes (Basel)*. **2023**, *14*, 464.
59. Xie, C.; Mao, X.; Huang, J.; Ding, Y.; Wu, J.; Dong, S.; Kong, L.; Gao, G.; Li, C. Y.; Wei, L. KOBAS 2.0: a web server for annotation and identification of enriched pathways and diseases. *Nucleic Acids Res* **2011**, *39*, W316-322.
60. Livak, K. J.; Schmittgen, T. D. Analysis of relative gene expression data using real-time quantitative PCR and the 2(-Delta Delta C(T)) Method. *Methods (San Diego, Calif.)* **2001**, *25*, 402–408.